

Change of Zonal Flow Spectra in the JIPP T-IIU Tokamak Plasmas

Y. Hamada, T. Watari, O. Yamagishi, A. Nishizawa, K. Narihara, Y. Kawasumi, T. Ido, M. Kojima, K. Toi, and the JIPP T-IIU Group

National Institute for Fusion Science, Toki, 509-5292, Japan

(Received 5 October 2006; revised manuscript received 9 April 2007; published 10 August 2007)

When Ohmically heated low-density plasmas are additionally heated by higher-harmonics ion-cyclotron-range-of-frequency heating, heated by neutral beam injection, or strongly gas puffed, the intensity of zonal flows in the geodesic acoustic mode frequency range in the tokamak core plasma decreases sharply and that of low-frequency zonal flow grows drastically. This is accompanied by a damping of the drift wave propagating in the electron diamagnetic drift direction, turbulence by trapped electron mode (TEM), and the increase of the mode propagating to ion diamagnetic drift direction (ITG). In the half-radius region, TEM and high-frequency zonal flows remain intense in both OH and heated phases. ITG and low-frequency zonal flows grow in heated plasmas, suggesting a strong coupling between ITG and low-frequency zonal flow.

DOI: [10.1103/PhysRevLett.99.065005](https://doi.org/10.1103/PhysRevLett.99.065005)

PACS numbers: 52.35.Ra

Inverse spectral energy transfer from small-scaled drift wave eddies to large-scale sheared poloidal flows such as zonal flows is regarded as one of the key issues of plasma confinement [1–9] since these flows have a large effect on the plasma confinement through shearing of plasma turbulences [10]. Several computer simulations [4,5,7–9] and experiments using various diagnostics on various toroidal devices [11–20] have found that zonal flows have wide frequency spectrum from low frequency (LF) up to high frequency [HF, around geodesic acoustic mode (GAM) frequency range [21]]. For $T_e \gg T_i$ plasmas, the drift waves called trapped electron mode (TEM) and/or electron temperature gradient (ETG) mode are dominant [22,23], and the critical electron temperature gradient determined by gyrokinetic stability equations for TEM or ETG is found to be consistent with the observed electron temperature gradient [24–26]. For $T_i \geq T_e$ plasmas, ion temperature gradient (ITG) mode is dominant. Study of the difference in zonal flow spectra excited by various drift wave modes is important for experimental and theoretical study, since the frequency of zonal flow must be lower than that of turbulence to be effective in regulating turbulence [3].

One of the most powerful diagnostics for the study of these phenomena may be a heavy ion beam probe (HIBP), since slow zonal flows of order of diamagnetic drift velocity can be determined by E/B ($= -\nabla\Phi/B$) motion, through fast, local, and multipoint measurement of plasma potential (Φ) [11,15,18,20]. The existence of potential oscillations with poloidal mode number $m = 0$ and $300 V_{p-p}$ around 30 kHz in the low-density OH core plasma where $T_e \gg T_i$ was reported by our group in 1995 at the seventh International Toki Conference on Nuclear Fusion [11]. This was found using HIBP. Recently, the analysis was extended to a wide region of the plasma cross section [18,20]. It showed that the radial dependence of the frequency is in agreement with GAM

frequency, and the radial correlation length is about in the 1–2 cm range [18]. The existence of intense GAM oscillations near the $q = 1$ region in low-density OH plasmas was interpreted by Watari *et al.*, deriving the small damping factor of $\exp(-\tau q^2)$, where $\tau = T_e/T_i$ and q is a safety factor [27]. In this Letter, we present the first experimental results showing the drastic change of the zonal flow spectrum (transition of the dominance of HF zonal flows to LF zonal flows) accompanied by the change of the mode of drift wave turbulence.

The experiment was carried out in a JIPP T-IIU tokamak plasma with nearly circular cross section and with major and minor radii of 93 cm and 23 cm, respectively [28]. The main diagnostics are a YAG Thomson scattering (YAGTS) with 28 spatial measurement points and a 100 Hz repetition rate, a 10-channel ECE polychromator, a 6-channel FIR interferometer, and a charge recombination spectrometer using neutral beam injection (NBI) to obtain ion temperature profiles. We have two different ways of providing additional heating, nearly perpendicular neutral beam injection (NBI with the injection angle inclined only by 9 degrees in the codirection), and ion-cyclotron-range-of-frequency (ICRF) $3\omega_{ci}$ heating and current drive (H/CD) with a phased 12-strap antenna on the smaller major radius side.

The HIBP for the JIPP T-IIU tokamak facilitates the injection of a 50–500 keV thallium (Tl^+) beam of a few tens of micro-Amps and the detection of the secondary thallium beam (Tl^{++}) ionized in the plasma [11,18,29]. The change in the energy of the Tl^{++} beam and its intensity correspond to the local plasma potential and plasma density, respectively, where the ionization takes place (sample volume, SV). The position, size, and direction of alignment of 6 SVs of HIBP and 4 SVs (thick bars, 3 cm apart each other) of the 10-channel ECE polychromator are shown in Fig. 1(a). The HIBP's SVs are specified by three parameters: i.e., primary beam energy ($j = A, B, \text{ and } C$,

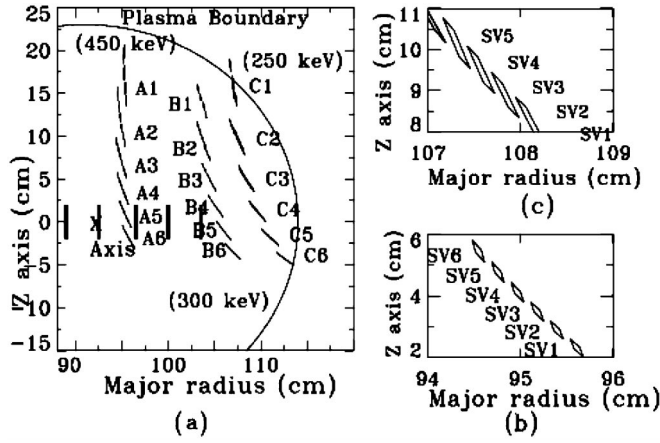


FIG. 1. (a) Location and direction of alignment of 6 SVs of the HIBP at 18 steps and 4 ECE SVs (thick vertical bars) out of 10 channel ECE polychromator measurement, discussed in this Letter. The label A stands for the beam energy of 450 keV, label B for 300 keV, and label C for 250 keV. (b) Shape and positions for SVs at step A4 and (c) is for C2.

for 450, 300, and 250 keV, respectively, under a toroidal magnetic field of 3 T, poloidal injection angle ($k = 1-6$), and input slit number of an energy analyzer ($l = 1-6$). The beam energy is fixed during one plasma discharge. A set of partial lines, designated by 2 labels (energy and injection angle) like A2, is called “a step” in this Letter. Figures 1(b) and 1(c) show an expanded view of what SVs look like at step A4 and step C2, respectively. The SVs are cylinders of about 2–4 mm in diameter, cut at a slant angle with a side view of a parallelogram. The length (the longer diagonal of the parallelogram, l_s) is about 5 to 15 mm along the beam trajectory, depending on the three parameters. The frequency bandwidth of the detector circuit at 3 db gain decrease is 300 kHz.

The experiments were carried out under the following conditions [18,20,30]: the plasma current is 200 kA with a safety factor q value around 4.3 and a toroidal field of 3 T. Since the attenuation of the injected thallium beam in the core region is very severe in the high-density plasma, the HIBP turbulence measurement of core plasma was only possible in plasmas below the average density of $3 \times 10^{13}/\text{cm}^3$.

Figure 2 shows the time behaviors of the radial profiles of plasma density and electron temperature (measured by YAGTS) and the result of the local stability calculations (radial profile of real ω and growth rate) using the measured density and electron temperature profiles. The average plasma density at the initial Ohmically heated phase is low and is about $1 \times 10^{13}/\text{cm}^3$. As shown in Fig. 2(a), the plasma is heated up to 1.1 keV in the core by Ohmic heating only. In this phase, the ion temperature may be estimated to be less than 1/4 of the electron temperature, because only electrons are heated by Ohmic heating in these experiments and the energy transfer from the electron to ions is small because of low plasma density.

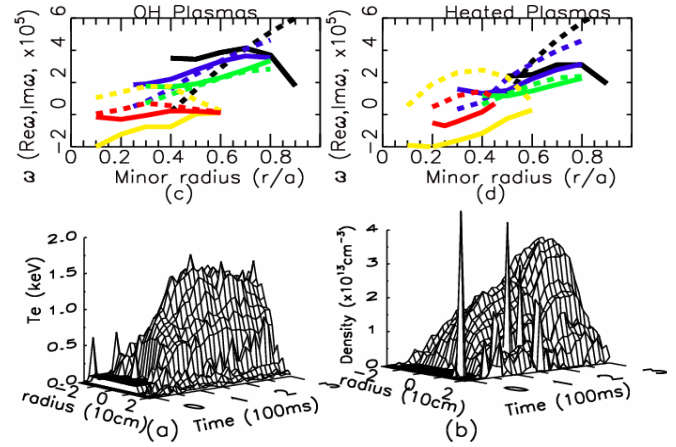


FIG. 2 (color online). Time behaviors of radial profiles of electron temperature (a) and plasma density (b) measured by 28-channel-YAG-laser Thomson scattering apparatus in the case of ICRF H/CD. (c) The real ω (solid line) and imaginary ω (dashed line) of the gyrokinetic stability calculations at low-density OH phase, (d) in heated phase. $T_e(r) = 1.23-1.28r'$ (in keV), $T_i(r) = 0.15(1-r')^2 + 0.02$, $n_e(r) = 1.43(1-r'^2)$ (in $/\text{cm}^3$) $+ 0.07$, $q(r) = 3.625r'^2 - 0.225r' + 0.9$, $r' = r/a_p$ are assumed for OH phase. For heated phase, $T_e(r) = 1.7-1.77r'$ (in keV), $T_i(r) = 0.5(1-r')^2 + 0.05$, $n_e(r) = 1.76(1-r'^2) + 0.23$. Black ($k_\theta \rho_i = 0.4$) and blue ($k_\theta \rho_i = 0.2$), green ($k_\theta \rho_i = 0.1$) curves are for TEM mode and red ($k_\theta \rho_i = 0.2$) and yellow ($k_\theta \rho_i = 0.4$) curves are for ITG mode. ρ_i is ion gyroradius.

At 160 ms, about half a MW $3\omega_{ci}$ H/CD ICRF power is injected for a duration of about 80 ms. The total plasma energy measured by plasma diamagnetism grows from 3 kJ to 8–9 kJ and the average plasma density rises to about $2 \times 10^{13}/\text{cm}^3$ due to both the strong plasma-surface (antenna) interaction during the heating period and to the gas puffing to suppress MHD oscillations. The electron temperature rises sharply at H/CD for about 10 ms and then increases only slowly due to the rapid increase of the plasma density, as is observed by YAGTS and ECE. Two center channels [the two left SVs shown in Fig. 1(a)] of the ECE emission show positive sawteeth in both the OH and heating phases. In the H/CD phase the amplitude of the sawtooth (peak to peak) increases about 5 times to about 20%. Accordingly the $q = 1$ circle (about 7 cm in diameter) does not change much during the ICRF fast-wave H/CD.

NBI heating has similar features, shown in Fig. 2: transient temperature rise followed by strong density rise due to particle fuelling by NBI, strong plasma-surface interaction, and gas puffing to avoid MHD activity. The peak ion temperature grows to about 0.6 keV, nearly half of the peak electron temperature near the end of the injection [29].

Figures 2(c) and 2(d) show the radial change of the real angular frequency (ω) and the growth rate of TEM and ITG in the OH phase and heated phase, respectively. These are calculated using linear gyrokinetic stability code GOBLIM under ballooning approximation [22,31]. The parameter of the plasma in the calculation is taken from the experimental values. The growth rate of TEM, propagating

in the electron diamagnetic drift direction, is heavily dependent on the wave number $k_\theta \rho_i$ and generally comparable to that of ITG mode in the core of low-density OH plasmas. In the heated phase, ITG becomes stronger and TEM almost disappears in the core. At half radius, TEM still has large growth rate even in the heated phase.

Figures 3 and 4 show 2D Fourier spectra of plasma potential and relative density fluctuations \tilde{n}_e/\bar{n}_e of the Fig. 2 discharge, at the rather steady phase of low-density Ohmic discharge from 100 ms to 150 ms and those spectra during the heating period from 180 ms to 230 ms, respectively. The SVs are at the position of A5 and aligned nearly poloidally. As shown in Fig. 3(c) and 4(c), the potential oscillations in the entire frequency range where signals are above noise level have almost all energy in the $k_\theta = 0$ component ($m = 0$). In addition, the phase difference between SVs is zero and the correlation length is short in the entire frequency range. We therefore consider these potential oscillations as due to LF and HF zonal flows. There is a significant difference in the potential spectra in the OH and heated phases, the decrease in the intensity of HF zonal flow being partly due to the increase of linear attenuation of GAM with the increase of ion temperature. In addition, we observed an increase in the level of the LF zonal flows between 0.2–20 kHz at the H/CD. We carefully controlled the gas puffing to suppress MHD oscillations before and during heating, and there are no MHD activities which affect strongly HIBP potential measurement. The ratio of the integral intensity of HF zonal flow from 20 kHz to

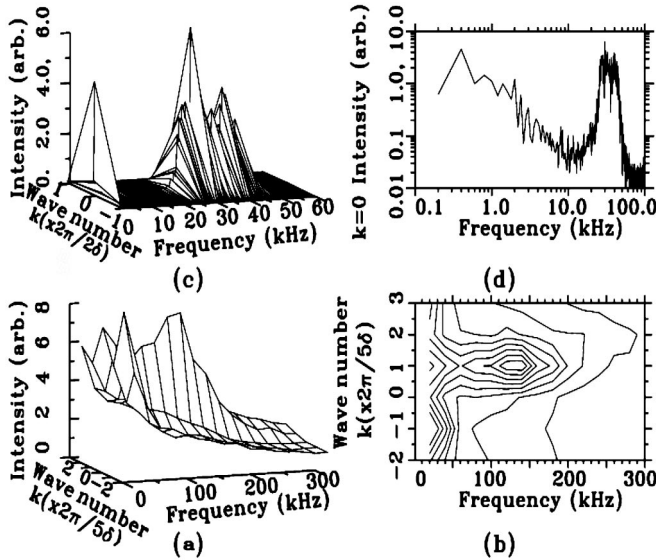


FIG. 3. (a) Surface plot and (b) contour plot of 2D Fourier spectra of normalized electron density \tilde{n}_e/\bar{n}_e . (c) Surface plot, (d) frequency spectrum of $k = 0$ component, of 2D Fourier spectra of plasma potential in the core region of A5 in the Ohmic phase (100–150 ms). δ (distance between SV1 and SV2) is about 7 mm (about 6 mm poloidally separated and 4 mm radially separated). In 2D spectrum, positive k number and positive frequency corresponds to the propagation to electron diamagnetic drift direction.

50 kHz, to the integral intensity of LF zonal flow from 200 Hz to 20 kHz, decreases from 10 in the Ohmic phase of Fig. 3(b) [20] to 1.4, while the total integral intensity decreases in the heated phase by a factor of 2.

There is a significant change in the density spectra in these plasmas. In the low-density OH plasmas, the dominance of the turbulence propagating in the electron diamagnetic drift direction with the wavelength larger than ion gyroradius ρ_i (we interpret this to be TEM) [22,23] is clearly observed in Fig. 3(a) and 3(b) at A5, and this phenomena is observed in a wide region from A6–A2, as can be expected from Fig. 2(c). We can observe in Fig. 3(b) small components at about 10–30 kHz, propagating in the ion diamagnetic drift direction (we interpret as ITG) in the OH phase. The wave number (k_l) measured by 6 SVs is $k_l = 2\pi l/L$, $l = -2$ to 3, $L = 5\delta$ where L is the total distance and δ is the distance between SVs. δ is about 6 mm at A5. The peak of observed TEM oscillations is at $l = 1$ (electron diamagnetic direction) and frequency is about 140 kHz. In the low-density OH phase, at A5 $k_l \rho_i = 0.1$ because the ion temperature is about 200 eV and a little larger growth rate for TEM can be expected from Fig. 2(c) for $l = 2$. However, the longer diagonal (l_s) of the parallelogram in Figs. 1(b) which is nearly parallel to poloidal direction and about 1 cm long, reduces the signal level of the wave with shorter poloidal wavelength. The reduction factor of this parallelogram is given by $\exp\{-(k_\theta l_s)^2/16.0\}$ [29], and we get significant attenuation of signals for $|l| \geq 2$.

In the heated phase, TEM is weak and LF oscillations at less than 50 kHz are greatly enhanced [Fig. 4(a) and 4(b)]. Those results are consistent with Fig. 2(d), larger growth rate of ITG, and negative growth rate for TEM at A5 in

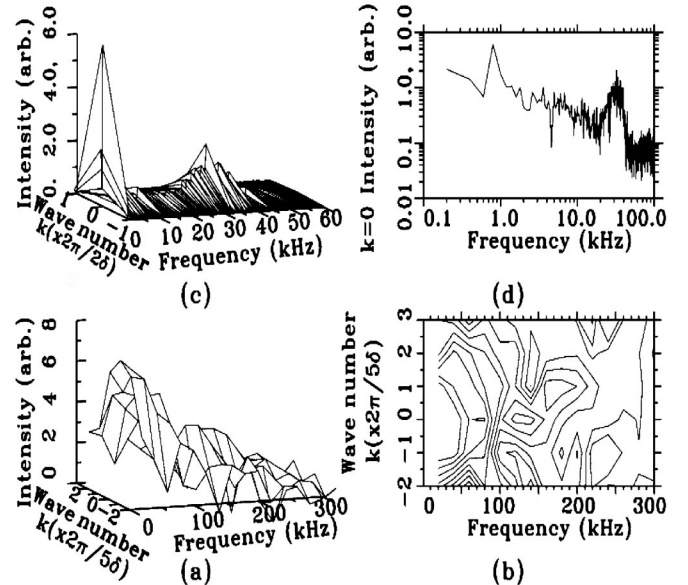


FIG. 4. The spectra during $3\omega_{ci}$ ICRF heating/CD (180–230 ms). The vertical scales of (a), (c), and (d) are the same with those of Fig. 3.

heated plasmas The intense LF oscillations near $\omega = 0$ are interpreted as the growth of ITG, in the heated plasmas and Doppler shifted to near zero or negative frequency (f) because of strong negative potential in the core. The reason of the presence of spectrum with positive k and f in Fig. 4(b) may be interpreted by the change of polarity of both negative F and k to positive values through the property of 2D Fourier density spectrum $S(k, \omega)$, $S(-k, -\omega) = S(k, \omega)$. The quasisteady electric potential at the core increases from about -1 kV to -1.5 kV by the heating. However, the accurate estimate of quasisteady local electric field at the core is future work.

The recent gyrokinetic flux tube simulations for $T_e \gg T_i$ plasmas by Dannert *et al.* [8] observed streamer phenomena in TEM turbulence. We observed low-amplitude (about 10%) streamerlike phenomena in the half-radius region of B3–B6 and a streamer of order of 50% \tilde{n}_e/\bar{n}_e in the region of 0.8–1.0 normalized radius (C1–C6) [30]. In the core region of A3–5 we cannot observe streamers. The existence of intense HF zonal flow that we observed n Fig. 3(c) is not reported in their paper. The spectrum of zonal flow of Fig. 4(d) is similar to that obtained by gyrokinetic simulation by Hahm *et al.* [5]. The spectrum is also very similar to the spectrum obtained in BES measurement by Gupta *et al.* [17]. This change in zonal flow spectrum during ICRF H/CD is similar to the change in the plasma with NBI heating and in the Ohmically heated high-density plasma generated by strong gas puffing.

At A2 and A3 with a larger minor radius, the HF zonal flows and TEM are strong in both the low-density OH and heated phases and a large increase of ITG and LF zonal flow is observed in the heated plasmas. The spectrum of zonal flows in the low-density Ohmic phase is almost the same as that of Fig. 3 (core region). Miyato *et al.* predicted using computer simulations that in the half-radius region HF zonal flows in the GAM frequency range would be dominant and have a broad spectrum in the ITG plasma [7], similar to our experimental observations. They explained the difference between the zonal flow spectra in the core region and half-minor region as due to the decrease of damping for larger q as is shown in $\exp(-q^2)$. In our case, intense TEM and ITG are observed even in the heated phase. Gyrokinetic ITG simulations by Angelino [9] yielded a result similar to Miyato *et al.* [7]. The behavior of zonal flow spectra in the TEM plasma ($T_e \gg T_i$) has not yet been investigated by global computer simulation, because much more computational time is needed to follow the rapid motion of the electrons along the magnetic field. In the future, results of long-time global simulation of TEM tokamak plasmas will be compared with our results. It should be mentioned that we cannot measure ETG with our HIBP and the effect of ETG on our study is our future work.

In summary, when the plasma is heated by ICRF fast wave or by NBI, or strongly gas puffed, the change of

dominance of the drift wave mode from TEM to ITG and that of zonal flow from HF to LF zonal flow are observed in the core. The entire spectrum of zonal flow in the heated phase is similar to that obtained by the ITG gyrokinetic simulation [5]. At half radius, TEM and HF zonal flow are intense in both phases and the growth of ITG and LF zonal flow is observed in the heated phase. From these results we can conclude that ITG mode is much more efficient in generating LF zonal flows than TEM.

The authors would like to thank Professor K. Itoh for fruitful discussions.

-
- [1] A. Hasegawa and M. Wakatani, Phys. Rev. Lett. **59**, 1581 (1987).
 - [2] Z. Lin *et al.*, Science **281**, 1835 (1998).
 - [3] T. S. Hahm *et al.*, Phys. Plasmas **6**, 922 (1999).
 - [4] K. Hallatchek and D. Biskamp, Phys. Rev. Lett. **86**, 1223 (2001).
 - [5] T. S. Hahm, Plasma Phys. Controlled Fusion **42**, A205 (2000).
 - [6] P. H. Diamond *et al.*, Plasma Phys. Controlled Fusion **47**, R35 (2005).
 - [7] N. Miyato *et al.*, Phys. Plasmas **11**, 5557 (2004).
 - [8] T. Dannert and F. Jenko, Phys. Plasmas **12**, 072309 (2005).
 - [9] P. Angelino *et al.*, Plasma Phys. Controlled Fusion **48**, 557 (2006).
 - [10] H. Biglari and P. H. Diamond, Phys. Fluids B **2**, 1 (1990).
 - [11] Y. Hamada *et al.*, Fusion Eng. Des. **34–35**, 663 (1997).
 - [12] M. G. Shats and W. M. Solomon, Phys. Rev. Lett. **85**, 4892 (2000).
 - [13] G. R. McKee *et al.*, Plasma Phys. Controlled Fusion **45**, A477 (2003).
 - [14] G. S. Xu *et al.*, Phys. Rev. Lett. **91**, 125001 (2003).
 - [15] P. M. Schoch *et al.*, Rev. Sci. Instrum. **74**, 1846 (2003).
 - [16] A. Fujisawa *et al.*, Phys. Rev. Lett. **93**, 165002 (2004).
 - [17] D. K. Gupta *et al.*, Phys. Rev. Lett. **97**, 125002 (2006).
 - [18] Y. Hamada *et al.*, Nucl. Fusion **45**, 81 (2005).
 - [19] G. D. Conway *et al.*, Plasma Phys. Controlled Fusion **47**, 1165 (2005).
 - [20] Y. Hamada *et al.*, Plasma Phys. Controlled Fusion **48**, S177 (2006).
 - [21] N. Winsor *et al.*, Phys. Fluids **11**, 2448 (1968).
 - [22] G. Rewoldt and W. M. Tang, Phys. Fluids B **2**, 318 (1990).
 - [23] F. Romanelli and S. Briguglio, Phys. Fluids B **2**, 754 (1990).
 - [24] W. Horton *et al.*, Phys. Plasmas **11**, 2601 (2004).
 - [25] D. R. Emst *et al.*, Phys. Plasmas **11**, 2637 (2004).
 - [26] A. G. Peeters *et al.*, Phys. Plasmas **12**, 022505 (2005).
 - [27] T. Watari *et al.*, Phys. Plasmas **12**, 062304 (2005).
 - [28] K. Toi *et al.*, Plasma Physics and Controlled Nuclear Fusion Research, 1992, Proceedings of the 14th International Conference Wurzburg, 1992 (IAEA, Vienna, 1993), Vol. 1, p. 519.
 - [29] Y. Hamada *et al.*, Nucl. Fusion **37**, 999 (1997).
 - [30] Y. Hamada *et al.*, Phys. Rev. Lett. **96**, 115003 (2006).
 - [31] O. Yamagishi *et al.*, Phys. Plasmas **14**, 012505 (2007).